DETERMINATION OF THE ABSOLUTE PHASE BETWEEN A FIELD AND ITS SECOND HARMONIC FOR USE IN A COHERENT CONTROL EXPERIMENT

A Thesis

Submitted to the Faculty

of

Purdue University

by

Christopher Alan Rupley

In Partial Fulfillment of the

Requirements for the Degree

of

Master of Science in Electrical and Computer Engineering

August 2004

This work is dedicated to my greatest teachers; my parents.

ACKNOWLEDGMENTS

I would first like to acknowledge my great appreciation to my major professor, Dan Elliott for giving my the opportunity to work on this project, and also for the numerous other opportunities he has given me to help enrich my education.

I would like to thank the professors who agreed to serve on my advisory committee, Mark Bell and Andrew Weiner. The contribution of their time is much appreciated.

I am also grateful for the other members of the lab who welcomed me in, took the time to share their knowledge with me, and helped keep things entertaining; Binh Do, Mevan Gunawardena, Art Mills, and Rekishu Yamazaki. I am especially thankful to Rekishu for the extensive effort he has put into helping me complete my project. Countless abstract and technical discussions and probing questions from him were of great help in completing this project.

PREFACE

In recent years, there has been growing interest in the field known as "Coherent Control." The continuing development of more stable, more powerful lasers has made this even more possible. Coherent control is a branch of science that studies the possibility of using known properties of coherent light, such as relative phase, to control various interactions. Applications range from controlling photo-ionization rate [1,2] to creating directional currents in semiconductors [3,4] to making measurements of atomic parameters [5] and controlling the products in photo-dissociation [6,7].

Many coherent control experiments will exploit the coherence properties between an optical field and its second harmonic. In a great deal of these, it is necessary to know the relative optical phase between these two fields at some point in space; typically where some interaction is taking place. In general, relative optical phase between two coherent beams of a single frequency can be easily determined by observing the interference between the two beams. This can analogously be done with a field and its second harmonic by first frequency doubling the fundamental frequency and then looking at the interference between that field and the original second harmonic field. However, in order to adapt this for use in some of these coherent control experiments, some additional considerations must be made. In this thesis project, we have developed a method to uniquely determine the phase difference between a field and its second harmonic at a specific point in space.

TABLE OF CONTENTS

LIST OF TABLES

LIST OF FIGURES

ABSTRACT

Rupley, Christopher Alan. M.S.E.C.E., Purdue University, August, 2004. Determination of the Absolute Phase Between a Field and its Second Harmonic For Use in a Coherent Control Experiment. Major Professor: Daniel S. Elliott.

We require knowledge of the relative phase between a field and its second harmonic at a certain point in space for use in a coherent control experiment. We will determine a method for measuring this phase difference in focused Gaussian beams. We will discuss the importance of various factors that have been overlooked in our previous experiments.

In order to make the relative phase measurement, a measurement will be made using a β-Barium Borate frequency doubling crystal that will allow us to determine the phase shift that occurs between a fundamental beam and its second harmonic during second harmonic generation. With this knowledge, and using various properties of focused Gaussian beams, we will be able to determine a scheme for finding the desired optical phase difference.

1. INTRODUCTION

1.1 Previous Work

Much work was done with this configuration by Z. M. Wang in working towards his Ph.D [8]. Wang adapted a type of photoelectron detector and employed it in various measurements of atomic rubidium. This new type of detector allowed for the measurement of many different atomic parameters in a single measurement as opposed to previous types of detectors that were used.

Wang was also able to measure further properties of atomic rubidium by running an experiment that employed quantum interference. He simultaneously excited both a one- and two-photon ionization in rubidium using a laser field and its second harmonic. This measurement produced a greatly asymmetrical electron angular distribution due to the quantum interference effects, and the degree of asymmetry was dependent on the relative phase of the two laser fields. Again, by fitting the theoretical data to experimental images, he was able to determine various parameters of atomic rubidium. He was able to measure the ratio of one-photon transition moments and the phase difference between p- and d-continuum waves. These allowed for a complete description of this transition.

1.2 Motivation for Current Work

While Wang's work was comprehensive in describing the interactions he was observing, some aspects of the experiment were overlooked that may affect the measurements that were made. This applies specifically to the phase difference between continuum waves found in the quantum interference experiment.

In order to determine the phase difference between p- and d-continuum waves, knowledge of the relative phase of the two optical fields present is required. The reason for this will be demonstrated in section (1.4). The method used to measure this was to let the fields propagate some distance from the interaction where a nonlinear crystal converted some of the fundamental beam into its second harmonic. The second harmonic has a definite phase relationship to that of the fundamental, so by measuring the interference between the original second harmonic field and the newly created second harmonic field, relative phase at the interaction can be determined.

When the original measurement was done, the phase difference between the two second harmonic beams was taken to be the same as the phase difference between the two fields at the interaction. What was neglected was the fact that there will be some phase difference that develops between the focused optical fields as they propagate into the far field region as well as when the second harmonic is generated.

The present work will be concerned with a calibration of the phase for the experiment performed by Wang. The result should be applicable to many types of coherent control experiments in which the relative phase between a field and its second harmonic must be known.

1.3 Experimental Overview

Since this work represents an extension of previous work performed by Z. M. Wang, many of the experimental conditions will be the same as is described in his Ph.D. thesis [8]. Much of it is repeated here for convenience as are the aspects that will be changed in order to improve his experiment.

The ultimate goal of this experiment is to determine the phase difference between p- and d-continuum waves in atomic rubidium. This will be done by looking at the quantum interference between one- and two-photon ionization processes. The photoelectron angular distribution that results from the process will be recorded,

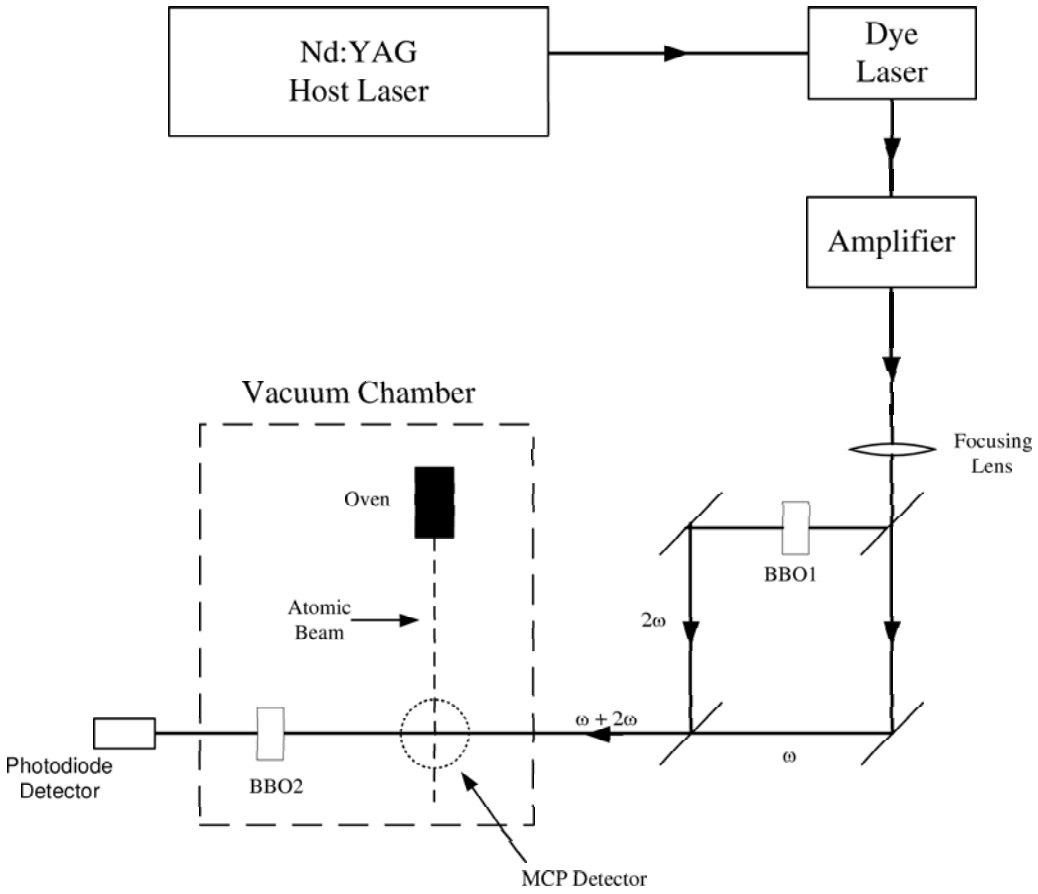

Fig. 1.1. Experimental setup for the measurement of the phase difference between p- and d-continuum waves in atomic rubidium

fitted with theory, and used to determine the phase difference. A diagram of the experimental setup is shown in figure (1.1).

A Q-switched Nd:YAG laser is used as a host to excite a tunable dye laser that produces a pulsed beam at the fundamental frequency with a wavelength of 560 nm. This will also be known as the visible beam. The beam is amplified and passes through a lens which will focus it close to where the optic/atom interaction will take place. Directly after the lens, the beam enters a Mach-Zehnder-like setup. In

one branch of the setup, the second harmonic of the fundamental beam is generated using a nonlinear β-Barium Borate (BBO) crystal. The second harmonic beam has a wavelength of 280 nm and will also be known as the uv beam. The two beams are recombined at the output side of the interferometer. This type setup allows for very good alignment and overlap of the two beams which is critical for a strong quantum interference signal to be detected.

Both the visible and uv beams will be focused to a spot inside a vacuum system close to the point where they will intersect a beam of rubidium atoms. The point where they intersect is labeled the interaction region. Located directly above the interaction is the Micro Channel Plate (MCP) detector which will collect images of the photoelectron angular distribution.

After traveling from the interaction region, the two beams will pass through another BBO crystal (BBO2) which will convert some of the fundamental beam to its second harmonic. The original second harmonic beam will pass through the crystal as well and it will interfere constructively or destructively with the newly generated second harmonic. The magnitude of the resulting uv beam exiting the vacuum system is directly related to the relative phase of the two beams and will be measured using a photodiode. This is the essence of the Phase Detector.

1.4 Theoretical Photoelectron Angular Distribution

The measurement of the phase difference between the continuum waves will be accomplished through measurement of photoelectron angular distribution (PAD) due to a given laser field. A general theory for predicting the electron angular distribution of an atom was developed by Bebb and Gold [9]. The experiment was performed specifically using the ionization of atomic Rubidium by a two-color field consisting of a frequency and its second harmonic with crossed linear polarizations. The theory of Bebb and Gold was applied specifically to this condition by Wang and Elliott [10] and the resulting angular distribution is shown in equation (1.1).

$$W(\Theta,\Phi)=\frac{m\left|\vec{k}\right|}{8\pi^2\hbar}\sum_{i,j=\pm}\left|\frac{eE_o^{2\omega}exp(i\phi^{2\omega})}{2\hbar}O_{ij}^{(1)}+\frac{e^2(E_o^{\omega})^2exp(2i\phi^{\omega})}{4\hbar^2}T_{ij}^{(33)}\right|^2, \quad (1.1)$$

where E_o^{ω} and $E_o^{2\omega}$ refer to the electric field amplitudes of the fundamental field and its second harmonic, respectively, and ϕ^{ω} and $\phi^{2\omega}$ refer to the phase of the fundamental and second harmonic fields, respectively. The applicable spatial components of the one-photon transition moment, $O_{ij}^{(1)}$, are given by

$$O_{++}^{(1)} = \frac{-4\pi i}{\sqrt{6}}e^{i\xi_p}\left[-Y_{1,1}R_{3/2}+Y_{1,-1}\left(\frac{R_{3/2}+2R_{1/2}}{3}\right)\right] \quad (1.2)$$

$$O_{--}^{(1)} = \frac{-4\pi i}{\sqrt{6}}e^{i\xi_p}\left[Y_{1,-1}R_{3/2}-Y_{1,1}\left(\frac{R_{3/2}+2R_{1/2}}{3}\right)\right] \quad (1.3)$$

$$O_{+-}^{(1)} = \frac{-4\pi i}{\sqrt{3}}e^{i\xi_p}Y_{1,0}\left(\frac{R_{3/2}-R_{1/2}}{3}\right) \quad (1.4)$$

$$O_{-+}^{(1)} = \frac{4\pi i}{\sqrt{3}}e^{i\xi_p}Y_{1,0}\left(\frac{R_{3/2}-R_{1/2}}{3}\right). \quad (1.5)$$

The spatial components of the two-photon transition moments, $T_{ij}^{(33)}$, are given by

$$T_{++}^{(33)} = \frac{1}{3}e^{i\xi_s}Y_{0,0}S_{\bar{s}}-\frac{2}{3\sqrt{5}}e^{\xi_d}Y_{2,0}S_{\bar{d}} \quad (1.6)$$

$$T_{--}^{(33)} = \frac{1}{3}e^{i\xi_s}Y_{0,0}S_{\bar{s}}-\frac{2}{3\sqrt{5}}e^{\xi_d}Y_{2,0}S_{\bar{d}} \quad (1.7)$$

$$T_{+-}^{(33)} = \sqrt{\frac{2}{15}}e^{i\xi_d}Y_{2,1}S_{\Delta d} \quad (1.8)$$

$$T_{-+}^{(33)} = \sqrt{\frac{2}{15}}e^{i\xi_d}Y_{2,-1}S_{\Delta d}. \quad (1.9)$$

In the above equations, $Y_{l,m}$ is the spherical harmonic function, $\xi_{s,p,d}$ is the phase of the s, p, or d partial wave, and $R_{1/2,3/2}$ is the single-photon transition moment. The following substitutions were made.

$$S_{\bar{s}}=\frac{S_1+2S_2}{3};S_{\bar{d}}=\frac{5S_3+S_4+9S_5}{15};S_{\Delta d}=\frac{5S_3+S_4-6S_6}{15} \quad (1.10)$$

The terms S_{1-5} refer to the two-photon radial transition matrix elements. If the above substitutions are made into equation (1.1), it can be simplified into the following form.

$$
\begin{aligned}
W(\Theta,\Phi) \propto & \left| M_R e^{i\phi_{2\omega}-2i\phi_\omega} e^{i(\xi_p-\xi_d)} \frac{-4\pi i}{\sqrt{6}} \left[-Y_{1,1} + Y_{1,-1} \frac{1+2\frac{R_{1/2}}{R_{3/2}}}{3} \right] + \ldots \right. \\
& \left. \left[\frac{1}{3} e^{i(\xi_s-\xi_d)} Y_{0,0} \frac{S_{\bar{s}}}{S_{\bar{d}}} - \frac{2}{3\sqrt{5}} Y_{2,0} \right] \right|^2 \\
+ & \left| M_R e^{i\phi_{2\omega}-2i\phi_\omega} e^{i(\xi_p-\xi_d)} \frac{-4\pi i}{\sqrt{3}} Y_{1,0} \frac{1-\frac{R_{1/2}}{R_{3/2}}}{3} + \sqrt{\frac{2}{15}} Y_{2,1} \frac{S_{\Delta d}}{S_{\bar{d}}} \right|^2 \\
+ & \left| M_R e^{i\phi_{2\omega}-2i\phi_\omega} e^{i(\xi_p-\xi_d)} \frac{4\pi i}{\sqrt{3}} Y_{1,0} \frac{1-\frac{R_{1/2}}{R_{3/2}}}{3} + \sqrt{\frac{2}{15}} Y_{2,-1} \frac{S_{\Delta d}}{S_{\bar{d}}} \right|^2 \\
+ & \left| M_R e^{i\phi_{2\omega}-2i\phi_\omega} e^{i(\xi_p-\xi_d)} \frac{-4\pi i}{\sqrt{6}} \left[Y_{1,-1} - Y_{1,1} \frac{1+2\frac{R_{1/2}}{R_{3/2}}}{3} \right] + \ldots \right. \\
& \left. \left[\frac{1}{3} e^{i(\xi_s-\xi_d)} Y_{0,0} \frac{S_{\bar{s}}}{S_{\bar{d}}} - \frac{2}{3\sqrt{5}} Y_{2,0} \right] \right|^2 , \quad (1.11)
\end{aligned}
$$

where M_R is the relative magnitude of the one-photon process to that of the two-photon process. It can clearly be seen from equation (1.11) that in order to determine the continuum phase difference, $\xi_p - \xi_d$, from a fit to this equation, it is necessary to know the optical phase difference, $\phi_{2\omega} - 2\phi_\omega$. Many of the quantities of equation (1.11) have been previously determined by Wang and Elliott [10,11]. These quantities are shown in table (1.1).

Using equation (1.11) and the properties of the detector system used by Wang [8] it is possible to develop expected angular distributions and the corresponding images that will be detected. Some example calculated images are shown in figure (1.2).

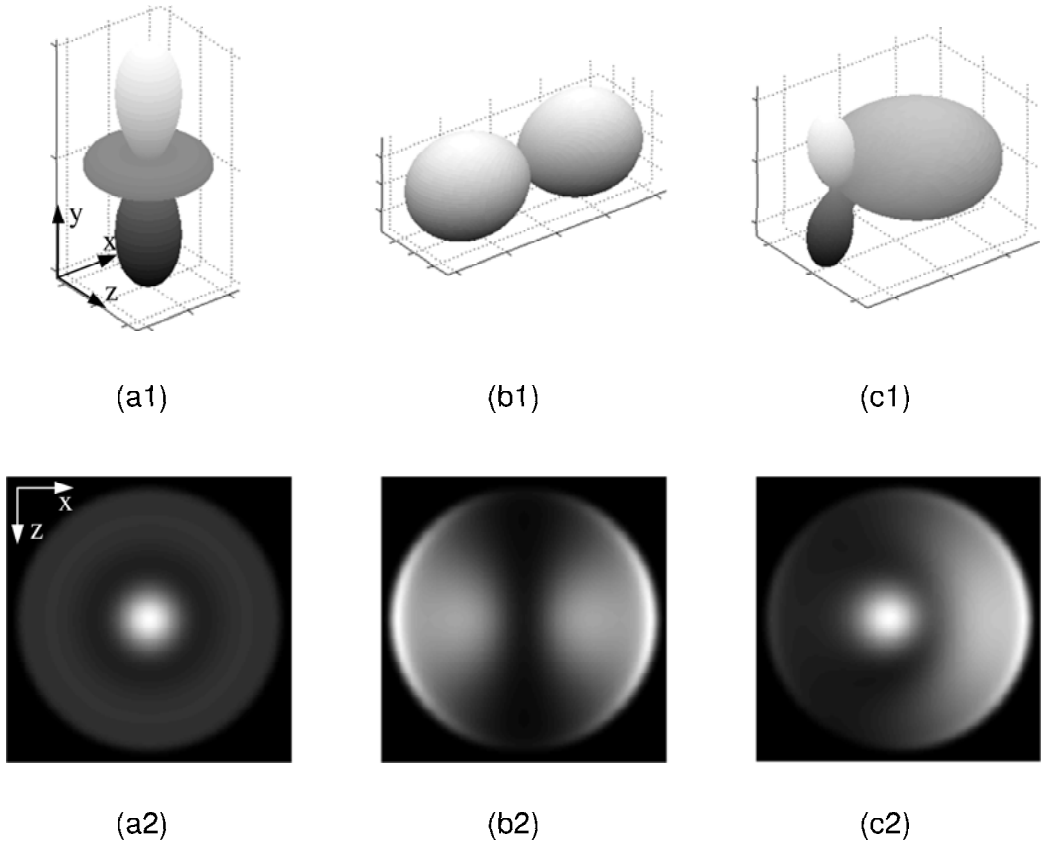

Fig. 1.2. Examples of various angular distributions, (x1), and their corresponding images, (x2), on the detector system. Images (a1,2) represent the result of excitation due to a field of wavelength 560 nm that is vertically polarized. Images (b1,2) are due to a horizontally polarized field at 280 nm. Images (c1,2) represent a result having both fields present.

Table 1.1
Values of known quantities used in equation (1.11)

Quantity	Value
$\frac{R_{1/2}}{R_{3/2}}$	1.96
$\frac{S_{\bar{s}}}{S_{\bar{d}}}$	-0.42
$\frac{S_{\Delta d}}{S_{\bar{d}}}$	-0.36
$\xi_s - \xi_d$	2.08

2. THEORY

Uniquely determining the phase difference between the p- and d- continuum waves requires knowledge of the relative optical phase of the two optical fields present at the interaction. The goal is to determine the optical phase difference, $\phi_{2\omega} - 2\phi_{\omega}$, between the fundamental field and its second harmonic at the interaction region. This can be done by using a second non-linear crystal to generate a co-linear second harmonic beam and then looking at the magnitude of the interference signal between the two second harmonic beams. The method makes use of the fact that, during second harmonic generation, the harmonic field has a definite phase relationship to that of the fundamental. In our experiment, both beams leave the interaction region and travel some distance, d, inside the vacuum system. They then pass through a BBO crystal where some of the visible beam is converted into its second harmonic. At the output of the BBO crystal there are now two second harmonic fields that will interfere constructively or destructively depending on their relative phase. The amplitude of the interfering beams will go as the square of the cosine of the phase difference between them. Therefore, by measuring the amplitude of the interference signal, the relative phase between the visible and uv fields at the interaction region can be determined.

Careful consideration must be made with respect to two things when using this method. The first is that, as these two focused Gaussian beams travel from their focus into the far-field, a phase difference will develop between them. The second is that there will be some phase difference between the visible beam and the second harmonic that is created from it within the BBO. If these are both accounted for, the optical phase difference at the interaction region can eventually be determined correctly.

2.1 Clarification of Coordinate Systems

In performing this experiment, it is necessary to define and adhere to a coordinate system in order to avoid confusion. In most cases, it is convenient to define the coordinates with respect to the traveling optical beam. For these cases, a coordinate system is defined in the following way. The positive z-axis points in the direction of the beam's propagation. The positive y-axis is normal to or up from the optical table, and the x-axis is located accordingly to create a right-handed coordinate system.

When dealing with crystal structures, it is often more convenient to define a coordinate system that coincides with the particular axes of the crystal. The type of crystal that is under study is a uniaxial crystal, which means that light polarized along one axis experiences a different index of refraction than does light polarized along the other two. This axis will be designated the optic axis and light polarized along it will be said to be experiencing an extraordinary refractive index. Light polarized along either of the other two axes will be experiencing an ordinary refractive index. In a crystal, it is customary to designate the optic axis as the Z-axis, which means that the X- and Y-axes will be used to designate the ordinary axes. For our purposes, the X- and Y-axes will be interchangeable.

The convention used here is to designate the laboratory coordinates in lower case (x, y, z) and the crystal coordinates in upper case (X, Y, Z). A diagram of these coordinates is shown in figure(2.1).

2.2 Shift During Propagation

We can consider the visible and uv beams to be focused Gaussian beams. In our reference frame, these beams are traveling in the $+z$ direction and the beams are focused at the point $z = 0$. The focal point is placed before the interaction region, located at the point $z = z_i$, for reasons discussed below. The second BBO doubling crystal is located some distance, d, after the interaction region. Refer to figure (2.2) for an illustration of terms used.

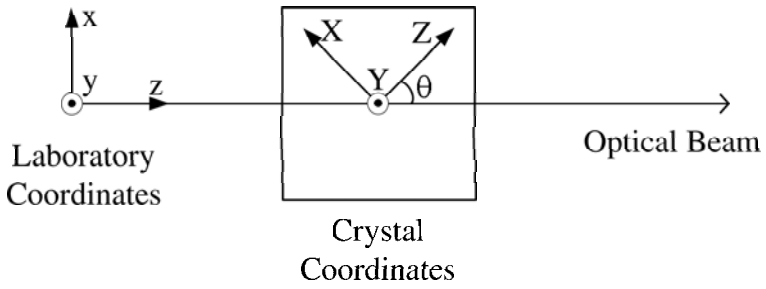

Fig. 2.1. Diagram showing the two types of coordinate systems used as viewed from above. Coordinates in lower case are defined with respect to the laboratory environment and coordinates in upper case are defined with respect to the crystalline axes.

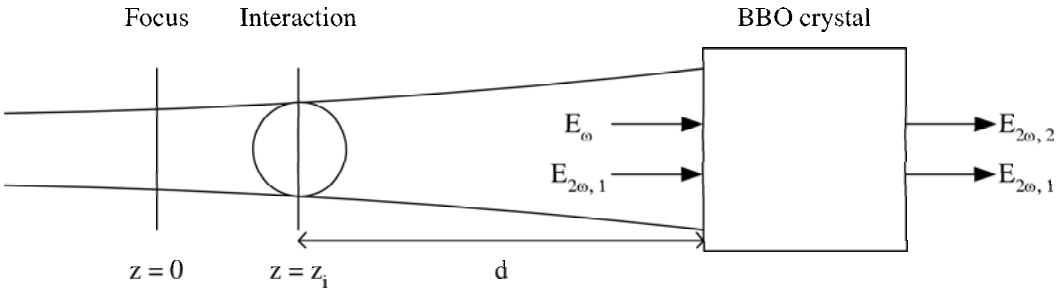

Fig. 2.2. Illustration of the method used to determine the Optical Phase Difference at the interaction region

If we assume an electric field of the form $E(z) = E_o e^{i\phi(z)}$ then, for a Gaussian beam, the phase changes with propagation according to [12]

$$\phi(z) = -kz + \arctan\left[\frac{z}{z_o}\right], \tag{2.1}$$

where k is the wave vector of the beam, and z_o is the beam's confocal parameter. It should be noted that a second harmonic beam will have both the same focal point and the same value of z_o as the fundamental wave from which it was created [13].

We are ultimately interested in determining the value of the optical phase difference at the interaction region, $\Delta\phi_i = \phi_{2\omega} - 2\phi_\omega$. We define the change in phase between the two fields as they travel the distance to the BBO crystal as the phase difference between the fields at the crystal, $\Delta\phi_d$, minus the phase difference at the interaction region, $\Delta\phi_i$. This is equal to the change in phase of the visible beam minus the change in phase of the uv beam over that distance.

$$\Delta\phi_d - \Delta\phi_i = \Delta\phi_{2\omega} - 2\Delta\phi_\omega \tag{2.2}$$

In the above equation, $\Delta\phi_{2\omega}$ and $\Delta\phi_\omega$ can be determined by using the fact that these are focused Gaussian beams and they obey equation (2.1). Phase difference during propagation due to dispersion can be ignored since the two beams are traveling in a high vacuum environment which can be considered effectively free from dispersion.

Knowing this, $\Delta\phi_{2\omega}$ in equation (2.2) can be found.

$$\Delta\phi_{2\omega} = \phi_{2\omega}|_{z=z_i+d} - \phi_{2\omega}|_{z=z_i} \tag{2.3}$$

$$= \left[-k_{2\omega}(z_i + d) + \arctan\frac{z_i + d}{z_o}\right] - \left[-k_{2\omega}z_i + \arctan\frac{z_i}{z_o}\right] \tag{2.4}$$

Similarly,

$$\Delta\phi_\omega = \left[-k_\omega(z_i + d) + \arctan\frac{z_i + d}{z_o}\right] - \left[-k_\omega z_i + \arctan\frac{z_i}{z_o}\right]. \tag{2.5}$$

Since the uv beam has double the frequency of the visible beam, the wave vectors of the two beams are related by: $k_{2\omega} = 2k_{\omega}$. Accounting for this and substituting equations (2.4) and (2.5) into equation (2.2) yields

$$\Delta\phi_d - \Delta\phi_i = -\arctan\frac{z_i + d}{z_o} + \arctan\frac{z_i}{z_o}. \tag{2.6}$$

As d becomes large relative to z_o, the first term of equation (2.6) approaches $-\frac{\pi}{2}$. In our experimental setup, z_o is on the order of a few millimeters and d is about 40 cm and so this approximation will be made.

If we look at the second term of equation (2.6), we can see the reason for placing the focus slightly before the interaction region. The arc tangent function is rapidly varying when its argument approaches zero, therefore, choosing a value of z_i that is very small could potentially introduce a large amount of error in the final calculation of the phase difference. If z_i is chosen to be a bit larger, small errors in the location of the focus will have less of an overall impact on the phase measurement. In the end, the phase difference will have to be adjusted by this factor.

2.3 Shift During Second Harmonic Generation

In second harmonic generation (SHG), the newly generated field will have a definite phase relationship to that of its driving field. In general, this phase difference is non-zero and so it must be determined in order for us to determine the phase relationship between the visible and uv beams at the interaction. To calculate this, we must look at the second harmonic generation process.

In our experiment, a second harmonic field is generated using the nonlinear crystal β-Barium Borate or BBO. It is classified as a negative uniaxial crystal and it has a crystal class of $3m$. The crystal used was cut for Type I SHG at a phase matching angle that corresponds to the fundamental wavelength of 560nm. In Type I SHG, the fundamental and second harmonic fields are linearly polarized and perpendicular to each other. The phase matching angle, θ, is the angle between the optic axis of

the crystal and the propagation direction of the optical beam at which both the fundamental and second harmonic beams have the same phase velocity within the crystal. In BBO, this angle is 44.4° for a fundamental wavelength of 560nm.

2.3.1 Nonlinear Optics Background

The nonlinear effects arise from the fact that the material exhibits a non-linear susceptibility. In general, the polarization of a material, P, may be described by

$$P = \epsilon_o \chi E, \tag{2.7}$$

where χ is known as the susceptibility of the material, which may be non-linear. Expanding equation (2.7) for the case of a non-linear susceptibility yields

$$\begin{aligned} P &= P^{(1)} + P^{(2)} + P^{(3)} + ... \\ &= \epsilon_o \chi^{(1)} E + \epsilon_o \chi^{(2)} E^2 + \epsilon_o \chi^{(3)} E^3 + ... \end{aligned} \tag{2.8}$$

We will be primarily concerned with the second order susceptibility, $\chi^{(2)}$, since it contributes to second harmonic generation and it offers a far greater contribution than do all other higher order terms. In general, $\chi^{(2)}$ is a second order tensor. Under certain symmetry conditions and using the relation $d_{ijk} = \frac{1}{2}\chi^{(2)}_{ijk}$, equation (2.8) can be written in the following condensed form which accounts for all possible orientations. [14]

$$\begin{bmatrix} P_X \\ P_Y \\ P_Z \end{bmatrix} = 2 \begin{bmatrix} d_{11} & d_{12} & d_{13} & d_{14} & d_{15} & d_{16} \\ d_{21} & d_{22} & d_{23} & d_{24} & d_{25} & d_{26} \\ d_{31} & d_{32} & d_{33} & d_{34} & d_{35} & d_{36} \end{bmatrix} \begin{bmatrix} E_X^2 \\ E_Y^2 \\ E_Z^2 \\ 2E_Y E_Z \\ 2E_X E_Z \\ 2E_X E_Y \end{bmatrix}, \tag{2.9}$$

where E_i is the magnitude of the electric field polarized in the i direction. For a fixed polarization and propagation direction, equation (2.9) may be further abbreviated to the form

$$P^{(2)}(z,t) = 2d_{eff}E^2(z,t). \tag{2.10}$$

If we assume an electric field of form, $E(z,t) = \frac{1}{2}\left[Ee^{i(\omega t-kz)} + c.c.\right]$, and take the square of it, equation (2.10) becomes

$$P^{(2)} = 2d_{eff}\left[E^2e^{2i(\omega t-kz)} + c.c. + 2\left|E\right|^2\right]. \tag{2.11}$$

This nonlinear polarization consists of two parts. One part consists of a field oscillating at twice the original frequency, $2d_{eff}\left[E^2e^{2i(\omega t-kz)} + c.c.\right]$, which is responsible for second harmonic generation. The other part, $2d_{eff}\left[2\left|E\right|^2\right]$, contributes to what is known as optical rectification. It can be seen that this is a polarization that does not vary with time.

2.3.2 Second Harmonic Generation Process

We now want to relate the electric field of the fundamental beam entering the crystal to the second harmonic that is generated. This can be done through use of Maxwell's equations and the wave equation.

$$-\nabla^2E + \frac{1}{c^2}\frac{\partial^2}{\partial t^2}E = \frac{-4\pi}{c^2}\frac{\partial^2P}{\partial t^2} \tag{2.12}$$

By using an electric field of the form $E_\omega(z,t) = \frac{1}{2}\left[Ee^{i(\omega t-kz)} + c.c.\right]$ and equation (2.10), and by making the approximations of perfect phase matching and an undepleted fundamental beam, equation (2.12) reduces to [15]

$$E_{2\omega} = -i\omega\sqrt{\frac{\mu_o}{\epsilon}}d_{eff}E_\omega E_\omega L. \tag{2.13}$$

In the above equation, ω is the fundamental frequency, μ_o is the magnetic susceptibility of free space, ϵ is electric permeability of the crystal, and L is the length

of the crystal. The amplitudes of the second harmonic and fundamental fields are given by $E_{2\omega}$ and E_{ω}, respectively. Also, d_{eff} is defined as half of the second order nonlinear susceptibility. According to Eimerl [16], in crystal of class $3m$, d_{eff} can be found by

$$d_{eff} = d_{31}\sin\theta - d_{22}\cos\theta\sin 3\phi, \tag{2.14}$$

where θ is the angle between the beam's wave vector and the crystalline Z-axis and ϕ is the angle between the wave vector and the crystal's X-Z plane. The crystal used for this experiment is cut, for a beam with normal incidence to the surface, with angles of $\theta = 44.4^{\circ}$ and $\phi = 0^{\circ}$.

From equation (2.13), it can be seen that the phase of the second harmonic field differs from that of the fundamental due to the $-i$ factor in equation (2.13). This phase may also be affected by the sign on d_{eff} which may be either positive or negative, and depends on the relative orientation between the crystal's optic axis and beam direction. Overall, this correlates to a phase shift during SHG of either $-\frac{\pi}{2}$ or $+\frac{\pi}{2}$, as is demonstrated in equation (2.15).

$$\begin{aligned} e^{i\phi_{2\omega}} &= -i\cdot e^{i2\phi_{\omega}} = e^{i(2\phi_{\omega}-\frac{\pi}{2})} \quad \text{for} \quad d_{eff} > 0 \\ e^{i\phi_{2\omega}} &= +i\cdot e^{i2\phi_{\omega}} = e^{i(2\phi_{\omega}+\frac{\pi}{2})} \quad \text{for} \quad d_{eff} < 0 \end{aligned} \tag{2.15}$$

The phase of the second harmonic wave is denoted by $\phi_{2\omega}$, and the phase of the fundamental is ϕ_{ω}. Combining this with the result of section (2.2) yields an overall phase shift from the beam's focus to the phase detector of either 0 or π. In order to resolve this ambiguity, we must determine the sign of d_{eff}.

It can be seen in equation (2.11) that the term d_{eff} is common to both the second harmonic generation and the optical rectification processes. Therefore, if the sign of d_{eff} can be determined by measuring the optical rectification, then it will also be known for the second harmonic generation process.

2.3.3 Optical Rectification

Optical rectification is the process of generating a DC electric field from a time-varying optical field. An expression for the polarization that arises from an optical rectification process was derived in section (2.3.1).

$$P_{DC}^{(2)} = 2d_{eff}\left|E\right|^2. \tag{2.16}$$

In our experiment, linearly polarized light is used in a Type I phase matching configuration and this generates both a second harmonic signal and an optical rectification signal. The two generated fields will have polarization perpendicular to that of the input field. Let us assume that the input field is polarized in the y-direction and that it is intersecting the crystal's optic axis at some angle, θ. The exact orientation of the crystal axes is not known, so an orientation is assumed for the purposes of this derivation. The angle that the wave vector makes with the crystal's optic axis is known, however, due to the phase matching condition for generation of second harmonic. The relative orientations of the crystalline axes and the laboratory coordinates are shown in figure (2.3).

Since the beam is propagating in the z-direction, we can arrive at an expression for the resulting DC polarization, written in the laboratory coordinate system. In order to obtain this expression, we begin with the equation relating polarization to electric field that was given in equation (2.9). For a specific crystal class, certain symmetry conditions may restrict certain values in the d_{ij} matrix to be zero or equal to other values in the matrix. Since we are considering specifically a BBO crystal we may use the reduced form for crystals of class $3m$, of which BBO is a member [14].

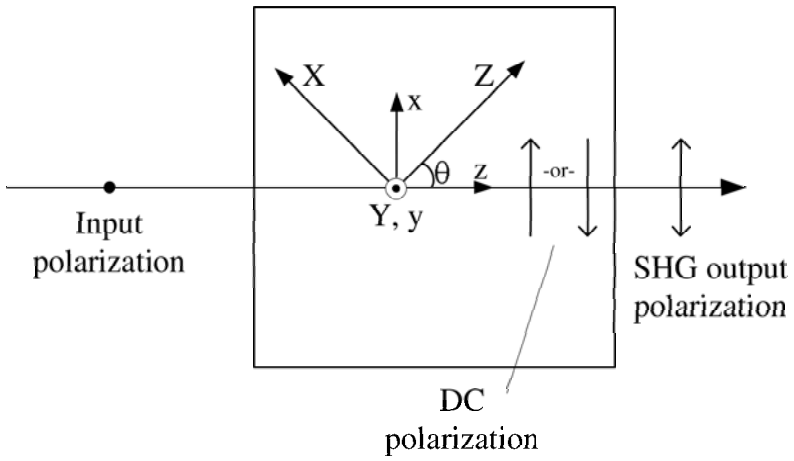

Fig. 2.3. Diagram of the relative orientations of the crystal and laboratory coordinate systems

$$\begin{bmatrix} P_X \\ P_Y \\ P_Z \end{bmatrix} = 2 \begin{bmatrix} 0 & 0 & 0 & 0 & d_{15} & -d_{22} \\ -d_{22} & d_{22} & 0 & d_{15} & 0 & 0 \\ d_{31} & d_{31} & d_{33} & 0 & 0 & 0 \end{bmatrix} \begin{bmatrix} E_X^2 \\ E_Y^2 \\ E_Z^2 \\ 2E_Y E_Z \\ 2E_X E_Z \\ 2E_X E_Y \end{bmatrix}. \tag{2.17}$$

Note that the indices are given in terms of the crystal coordinate axes. Since the input field consists only of an electric field linearly polarized in the Y-direction, equation (2.17) reduces to

$$\begin{aligned} P_Y &= 2d_{22}E_Y^2 \\ P_Z &= 2d_{31}E_Y^2. \end{aligned} \tag{2.18}$$

From this, we are interested only in the component of the polarization that is in the x-direction in our laboratory coordinate system. In other words, we want the component that is orthogonal to the input field and the propagation direction, which is the result of a Type I process. Transforming equation (2.18) into the laboratory coordinate system, the polarization in the x-direction is given by

$$P_x = 2d_{31}\sin\theta E_y^2, \tag{2.19}$$

and the DC polarization corresponding to this is

$$P_x = 2d_{31}\sin\theta |E_y|^2. \tag{2.20}$$

This result can be verified by comparing to equation (2.10) and recognizing that $d_{eff} = d_{31}\sin\theta$ for $\phi = 0$ from equation (2.14). Since we do not know the actual orientation of the crystal's positive Z-axis, we can say that we do not know the sign of $\sin\theta$, and we therefore do not know the sign of d_{eff}. The problem of finding the sign of d_{eff} now comes to determining the direction of the DC polarization that is developed in the crystal.

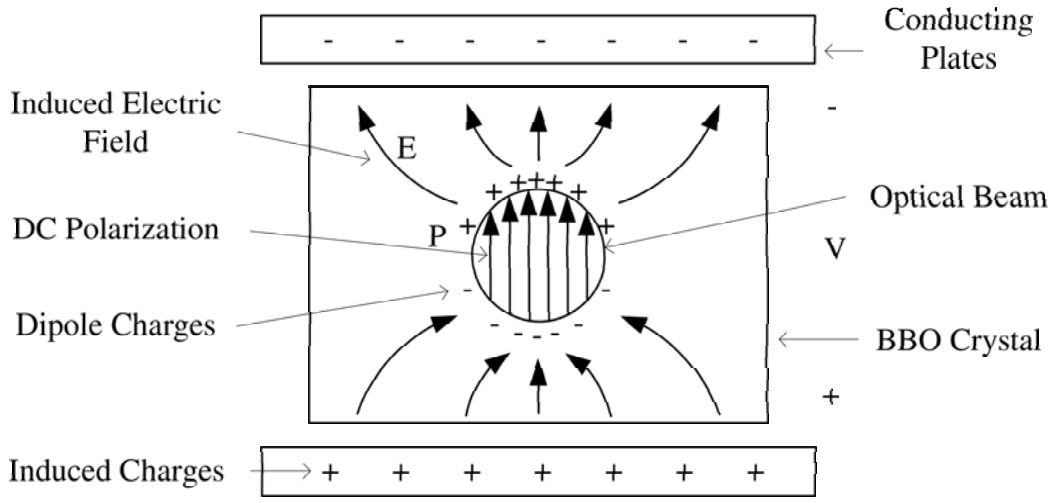

Fig. 2.4. Method used to detect the polarization direction. The DC polarization causes a separation of charge within the crystal which, in turn, induces charges on the conducting plates. The difference in charge on the plates corresponds to a voltage and the direction of the voltage drop can be used to find the polarization direction.

In order to measure this DC polarization, conducting electrodes are placed on the sides of the crystal perpendicular to the expected DC polarization vector. The polarization will be developed within the area of the laser beam in the crystal. This polarization corresponds to some density of dipoles, all oriented in the same direction. Within the crystal, this will appear as a separation of charge with one edge of the laser beam appearing to have a positive charge and the other appearing to have a negative charge. These charges will induce opposite charges on the conducting electrodes, and thus there will be a voltage difference between the two electrodes which can be measured. An illustration of this is shown in figure (2.4).

There are two possible cases that may arise, corresponding to possible signs of d_{eff}. Either the measured voltage will correspond to a DC field which points in the positive x-direction or in the negative x-direction. It can be seen from equation

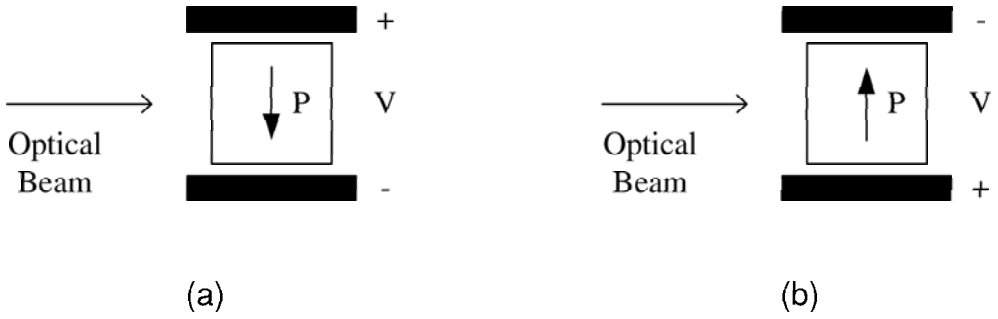

Fig. 2.5. Diagram showing the two possible results of an optical rectification measurement, including the resulting induced voltage.

(2.20) that a positive value of d_{eff} will yield a polarization in the positive x-direction and a negative value of d_{eff} will yield a polarization in the negative x-direction. An illustration of these two cases is shown in figure (2.5).

2.4 Theoretical Summary

We can accumulate all of the results from the current chapter to arrive at a compact expression for relating the phase difference at the interaction to the phase difference measured by the phase detector (PD). The result will depend on our measurement of the optical rectification signal. We wish to know the phase difference at the interaction, $\phi_{2\omega} - 2\phi_{\omega}$. We will measure some phase difference at the phase detector, and that will need to be adjusted for phase difference that develops due to propagation and to second harmonic generation. This is shown symbolically in equation (2.21).

$$\phi_{2\omega} - 2\phi_{\omega} = \Delta\phi_{PD} - \Delta\phi_{propagation} - \Delta\phi_{SHG}. \tag{2.21}$$

From section (2.2) we concluded that

$$\Delta\phi_{propagation} = -\arctan\frac{z_i+d}{z_o}+\arctan\frac{z_i}{z_o} \quad (2.22)$$

$$\approx -\frac{\pi}{2}+\arctan\frac{z_i}{z_o}. \quad (2.23)$$

And from section (2.3.2) we know

$$\Delta\phi_{SHG} = \mp\tfrac{\pi}{2} \quad \text{for} \quad d_{eff}\pm. \quad (2.24)$$

Inserting equations (2.23) and (2.24) into equation (2.21) yields

$$\phi_{2\omega}-2\phi_{\omega}=\Delta\phi_{PD}-\left[-\frac{\pi}{2}+\arctan\frac{z_i}{z_o}\right]-\left[\mp\frac{\pi}{2}\right] \quad \text{for} \quad d_{eff}\pm. \quad (2.25)$$

Full determination of the interaction phase difference requires knowledge of z_o and z_i which are known parameters in the experiment. It also requires knowledge of the sign of d_{eff} and a determination of that will be presented in the following chapter.

3. EXPERIMENT AND RESULTS

3.1 Measurement of Optical Rectification

We are interested simply in measuring the sign of d_{eff} and this can be done by measuring the direction of the DC electric field that is generated within the crystal. Since optical rectification is a second order process with a small nonlinear coefficient, a rather large electric field must be used in order to see some result; it must be comparable to that used to generate second harmonic fields. In our current setup we employ a Q-switched Nd:YAG laser capable of producing pulses with energies of up to 100 mJ of 10 ns duration at a wavelength of 532 nm. If we approximate the pulse as a square pulse in time, then this correlates to a peak power of 10 MW.

The DC electric field is measured by placing parallel conducting plates perpendicular to the field and then measuring the voltage that is induced across them. A diagram of the configuration used to make this measurement is shown in figure (3.1).

The crystal used in this experiment is a β-Barium Borate (BBO) that has an open face of 5mm$\times$4mm and is 5mm in length. It is oriented for Type I phase matching which means that the fundamental field and the harmonic field are polarized perpendicularly to one another. In this case, the fundamental field has a polarization along one of the crystal's ordinary axis, and the second harmonic, as well as the optical rectification signal, are created along the extraordinary axis.

In order to measure the direction of the optical rectification signal, the following configuration is used. The crystal is bounded with conducting plates on the sides perpendicular to the expected DC polarization direction, as was discussed in section (2.3.3). This configuration is equivalent to a parallel-plate capacitor where the crystal is the dielectric. A potential will develop between the plates when a DC field is present, and this voltage is expected to be on the order of a few hundred microvolts

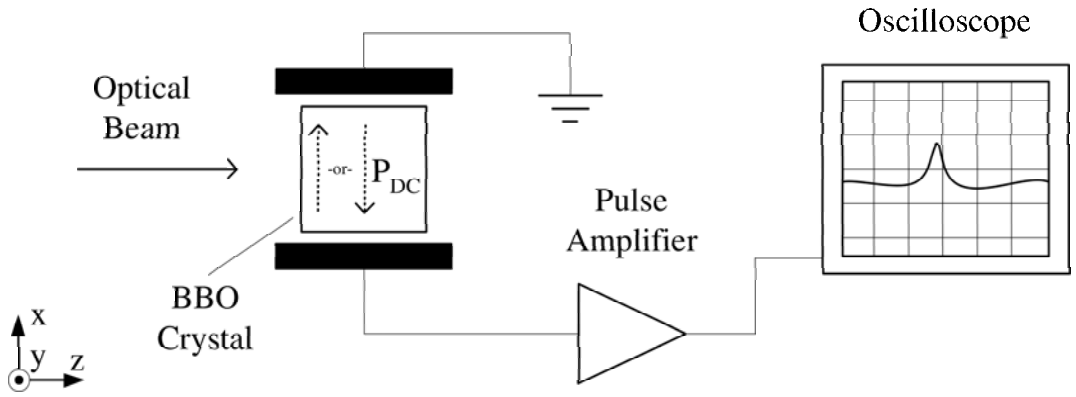

Fig. 3.1. Diagram of the experimental setup used to measure the optical rectification signal in a BBO crystal

due to the similarity of our experimental conditions to previous results [17]. This voltage will then be amplified and observed on an oscilloscope. A diagram of the experimental setup is shown in figure (3.1).

While the short duration pulses from the Nd:YAG laser do allow for higher peak power, they also make the DC measurement more difficult since the DC field is only present when the optical field is driving it. We therefore need a fast amplifier and detector that are capable of detecting the polarity of pulses of 10 ns duration. Other conditions on the amplifier are that it have high input impedance so as to match the impedance of the crystal capacitor at the input, and that a lower input capacitance is desirable [17]. Good high-frequency circuit techniques were used in the construction of the amplifier. Interconnection cable lengths were kept small, especially the connection between the crystal and the amplifier, which was approximately one inch.

A two-stage amplifier configuration was used. The first stage was constructed from a Burr-Brown model OPA656 operational amplifier. This is a high input impedance, unity-gain stable model with a 500 MHz gain-bandwidth product. A schematic diagram of the circuit constructed is shown in figure (3.2). The resistor connected between the non-inverting input and ground will set the input impedance. This resistor is also responsible for supplying the bias current to the op-amp. If we select this to have a large input impedance as required, on the order of megaohms, then the amplifier used must also have a very low bias current so that no significant voltage drop is apparent across the resistor due to the biasing. The OPA656 has a JFET-type input with a 2 pA input bias current. The amplifier circuit was configured to have an input impedance of 1.3 MΩ, an output impedance of 50 Ω and a gain of 2. This stage was used primarily to match the high impedance of the crystal to the 50 Ω impedance of the rest of the system.

The second stage of amplification was a Hamamatsu wide bandwidth amplifier model C6438-01. It has 50 Ω input and output impedances and a specified gain of 500. Both amplifiers are in a non-inverting configuration so as to avoid confusion as to the sign of the pulse. The amplifier system was interfaced to a 250 MHz

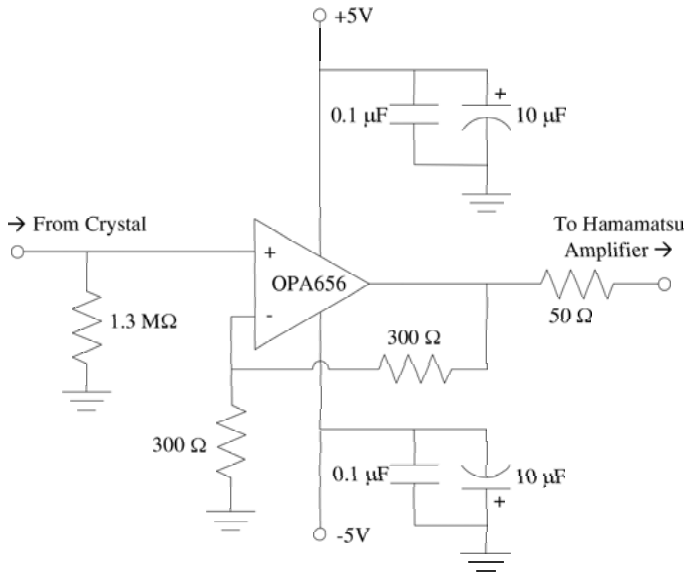

Fig. 3.2. Schematic diagram of the impedance matching amplifier connected between the crystal and the Hamamatsu amplifier.

oscilloscope so that the entire system had adequate bandwidth for a 10 ns pulse. The amplifiers provided an overall gain of 1000 which made it possible to detect the few hundred microvolt pulses on the oscilloscope after amplification.

3.2 Choice of Laboratory Coordinate System

Care must be taken in adhering the laboratory coordinate system. Since our goal is only to determine the sign of the term d_{eff}, any error in the orientation of the coordinates may have the result of changing the result to its opposite. All calculations and measurements must adhere to these coordinates for the same reason. These include the phase shift in moving to the far field, the orientation of the camera imaging system, the experimental image fitting program, and the orientation of the phase detection BBO.

Recall that the coordinate system is defined in the following way. The positive z-axis points in the direction of the beam's propagation, and the positive y-axis is normal to the optical table.

The first thing that must be accounted for is the orientation of the camera in the imaging system. The camera is positioned looking down on the interaction region, with the optical beam entering from the top of the image. Therefore, the collected image lies in the x-z plane with the origin in the upper left corner of the image.

This experiment uses an algorithm to fit the theoretical equations to the experimental images. Since the expected images will be asymmetric, it is important that the coordinate system used in the program coincides with that of the image that is passed to it. Therefore, care must be taken to insure that the orientations of the spherical harmonics in equation (1.11) match correctly. It should be noted that a change in optical phase of $\pi/2$ is equivalent to a flip of the image about the beam axis as demonstrated in figure (3.3).

Finally, the sign of d_{eff} that is measured will depend on the choice of coordinate system as well. Since we are using Type I phase matching in the second doubling crystal and the incoming electric field polarization is vertical (in the z-direction) we expect the polarization of the second harmonic as well as the optical rectification field to be horizontal (in the x-direction). Therefore, we expect

$$P_x^{(2)} = 2d_{eff} \left|E_y\right|^2 . \tag{3.1}$$

Determining the sign of d_{eff} now comes to determining if the DC polarization points in the positive or negative x-direction in our coordinate system.

3.3 Determination of Optical Rectification Direction and Optical Phase Shift

Before attempting to measure the optical rectification signal and thus the orientation of the crystal axes, the crystal was marked in such a way so that this knowledge

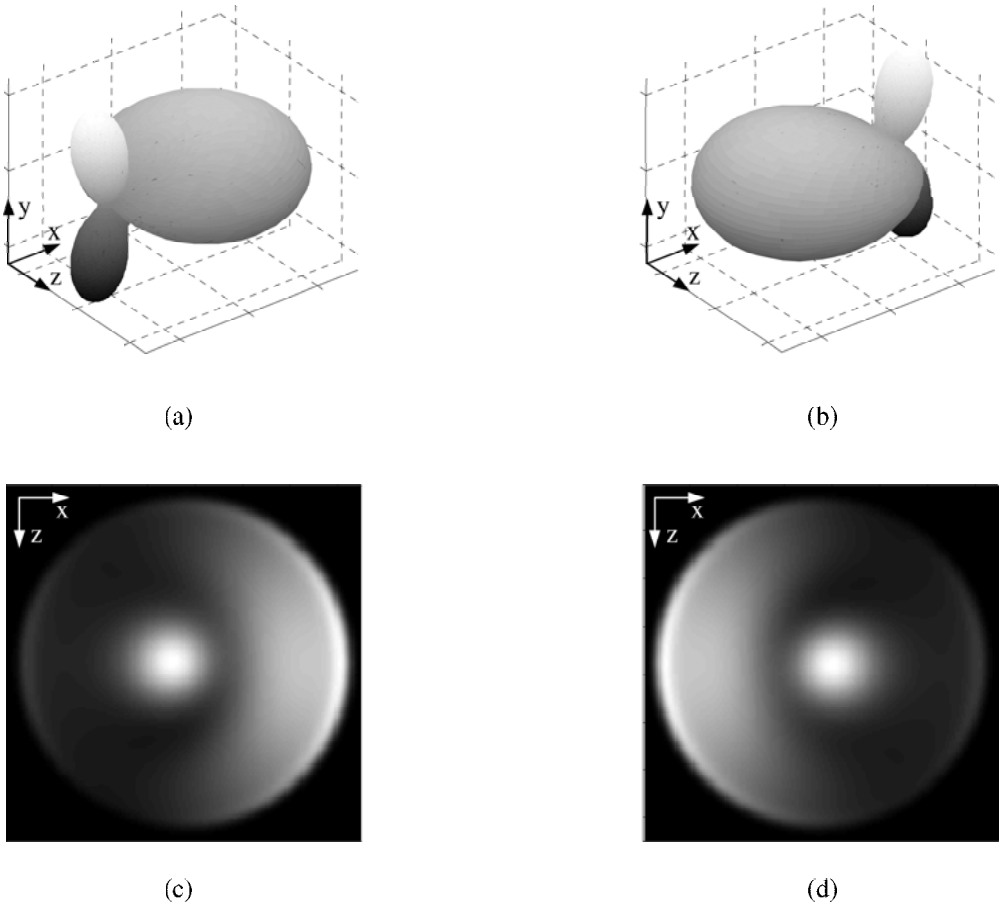

Fig. 3.3. Theoretical images demonstrating the differences in images corresponding to a π change in the optical phase. Image (a) is the 3D PAD for an optical phase difference of $\pi/2$ and (c) is the corresponding 2D detector image. Similarly, (b) and (d) are the result of an optical phase difference of $-\pi/2$.

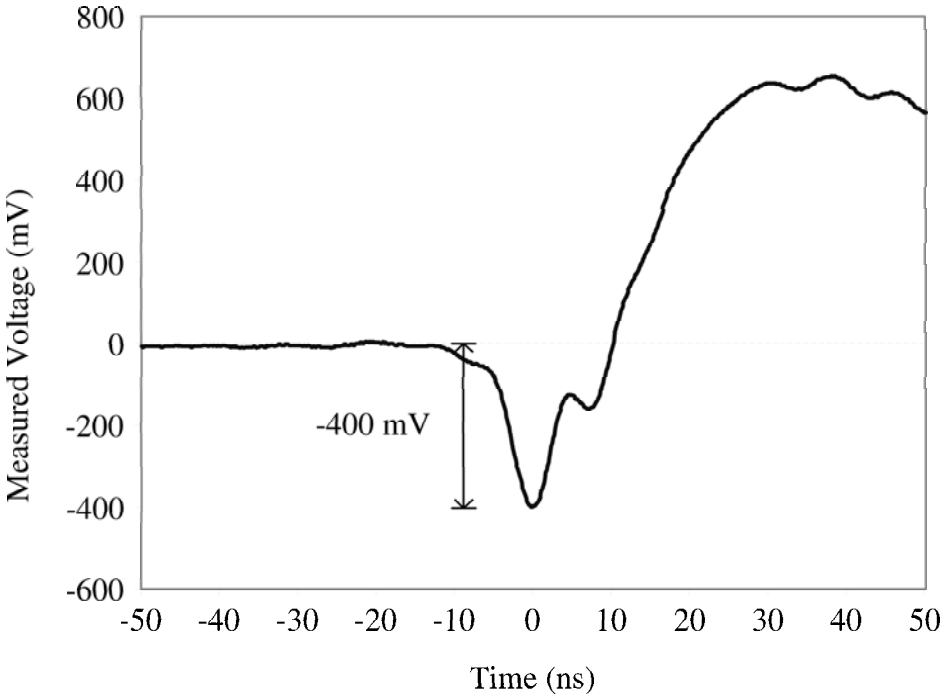

Fig. 3.4. Oscilloscope trace of a detected optical rectification signal. The pulse has a width of about 10 ns which correctly corresponds to the duration of the driving laser pulse.

could be preserved in transferring the crystal. An "input face" and a "top" of the crystal were designated.

The electrodes were attached to the crystal in such a way that the positive input to the amplifier was attached to the $-x$ side of the crystal and the negative or ground side was attached to the $+x$ side. The input laser was set to a pulse energy of 10 mJ at a wavelength of 532 nm. The oscilloscope was set to trigger on the signal from photodiode that was placed close to the crystal that was monitoring the input laser pulse. In order to account for small fluctuations, the scope was also set to average over as many as 500 pulses. The resulting trace is shown in figure (3.4).

The optical rectification pulse is clearly visible and it can be seen that it has a negative value. This means that the electrode on the $+x$ side had a higher potential,

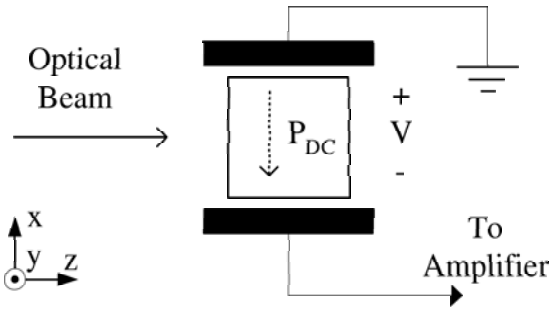

Fig. 3.5. Result of the optical rectification measurement showing the direction of the measured voltage drop and the corresponding DC polarization

and therefore the induced DC polarization points in the negative x-direction. An illustration of this result is shown in figure (3.5). From sections (2.3.2) and (2.3.3) we can conclude that this corresponds to a phase shift of $+\frac{\pi}{2}$. It should also be noted that directly after the OR pulse the oscilloscope trace shows another larger and longer pulse with opposite polarity of that of the OR pulse. The duration of this second pulse is on the order of a few microseconds. It is believed that this signal is due to a piezoelectric effect occurring within the crystal because of its relatively long duration and similarity to previous experimental results [17].

If we combine this final result with the result of section (2.4), we can arrive at a complete expression relating the phase at the interaction to that measured at the phase detector. The expression is valid for the relative orientation of the crystalline axes and the laboratory coordinate system used.

$$\phi_{2\omega} - 2\phi_{\omega} = \Delta\phi_{PD} + \arctan\frac{z_i}{z_o}. \tag{3.2}$$

In conclusion, we have developed a method to determine the phase difference between a field and its second harmonic at a certain point in space for focused Gaussian beams. We determined the phase difference that develops as the two

beams propagate. We also found the phase shift that occurs in the second harmonic generation process between the fundamental field and its second harmonic. This requires knowledge of the exact orientation of the crystal's optical axes. Measurement of these orientations was accomplished by measuring the direction of the optical rectification signal that accompanies the second harmonic generation process. The result was a complete expression relating the relative phase that was measured at the phase detector to the relative phase of the two beams at the interaction region.

LIST OF REFERENCES

LIST OF REFERENCES

[1] D. W. Schumacher and P. H. Bucksbaum. Phase dependence of intense-field ionization. *Physical Review A*, 54:4271–4278, 1996.

[2] D. W. Schumacher, F. Weihe, H. G. Muller, and P. H. Bucksbaum. Phase dependence of intense field-ionization - a study using 2 colors. *Physical Review Letters*, 73:1344–1347, 1994.

[3] E. Dupont, P. B. Corkum, H. C. Liu, M. Buchanan, and Z. R. Wasilewski. Phase-controlled currents in semiconductors. *Physical Review Letters*, 74:3596–3599, 1995.

[4] H. M. vanDriel, J. E. Sipe, A. Hache, and R. Atanasov. Coherence control of photocurrents in semiconductors. *Physica Status Solidi B-Basic Research*, 204:3–8, 1997.

[5] Z. M. Wang and D. S. Elliott. Determination of cross sections and continuum phases of rubidium through complete measurements of atomic multiphoton ionization. *Physical Review Letters*, 84:3795–3798, 2000.

[6] Y. Y. Yin, D. S. Elliott, R. Shehadeh, and E. R. Grant. 2-pathway coherent control of photoelectron angular-distributions in molecular no. *Chemical Physics Letters*, 241:591–596, 1995.

[7] B. Sheehy, B. Walker, and L. F. Dimauro. Phase-control in the 2-color photodissociation of hd+. *Physical Review Letters*, 74:4799–4802, 1995.

[8] Z. M. Wang. *Complete determination of atomic parameters in two-photon ionization and study of quantum interference with two-color laser fields.* PhD thesis, School of Electrical Engineering, Purdue University, 2001.

[9] H. B. Bebb and A. Gold. Multiphoton ionization of hydrogen and rare-gas atoms. *Phys. Rev.*, 143:1, 1966.

[10] Z. M. Wang and D. S. Elliott. Determination of the phase difference between even and odd continuum wave functions in atoms through quantum interference measurements. *Physical Review Letters*, 87:173001, 2001.

[11] Z. M. Wang and D. S. Elliott. Complete measurements of two-photon ionization of atomic rubidium using elliptically polarized light. *Physical Review A*, 62:053404, 2000.

[12] Joseph T. Verdeyen. *Laser Electronics.* Upper Saddle River, NJ: Prentice Hall, 1995.

[13] A. Ashkin D. A. Kleinman and G. D. Boyd. Second-harmonic generation of light by focused laser beams. *Phys. Rev.*, 145:338–379, 1966.

[14] Robert W. Boyd. *Nonlinear Optics.* San Diego, CA: Academic Press, 2003.

[15] Amnon Yariv. *Quantum Electronics.* New York, NY: Wiley Text Books, 1989.

[16] D. Eimerl, L. Davis, S. Velsko, E. K. Graham, and A. Zalkin. Optical, mechanical, and thermal-properties of barium borate. *Journal Of Applied Physics*, 62:1968–1983, 1987.

[17] P. A. Franken M. Bass and J. F. Ward. Optical rectification. *Phys. Rev.*, 138:A534–A542, 1965.